ISSN (Print) 1226-1750
ISSN (Online) 2233-6656
Journal of Magnetics 26(1), 41-49 (2021) https://doi.org/10.4283/JMAG.2021.26.1.041

Performance Evaluation of Image Characteristics by Changing Parameters in Brain T2 Weighted Neuroimages using MRiLab Simulation

Jun Lim[1], Seong-Hyeon Kang[1], Chan Rok Park[2], and Youngjin Lee[1]*

[1]*Department of Radiological Science, Gachon University, Incheon 21936, Republic of Korea*
[2]*Department of Radiological Science, Jeonju University, Jeollabuk-do 55369, Republic of Korea*

(Received 15 February 2021, Received in final form 11 March 2021, Accepted 12 March 2021)

Research has been conducted on techniques for adjusting magnetic resonance imaging (MRI) parameters to acquire images with better characteristics. In this study, we aim to confirm the optimal parameter values through quantitative evaluation and tendency analysis of T2 weighted images of the human brain acquired by adjusting the flip angle, number of excitations (NEX), and bandwidth (BW) using the user-friendly MRiLab simulation program. We also considered noise level and similarity evaluation parameters. According to the results, as NEX increases and BW decreases for a flip angle of 90°, the noise level and similarity evaluation improved, whereas they became less optimal beyond a 90° flip angle. Excessive parameter variation was found to cause additional noise and artifacts in such images, resulting in a deterioration of image clarity. Therefore, we confirmed that setting appropriate parameters is critical in magnetic resonance image acquisition.

Keywords : Magnetic resonance imaging (MRI), flip angle, Number of excitation (NEX) Bandwidth (BW), MRiLab simulation program, brain T2 weighted image

1. Introduction

Magnetic resonance imaging (MRI) refers to the generation of nuclear magnetic resonance phenomena to map hydrogen in tissues and form images of the interior of a human body. This technique has many advantages, such as being able to acquire three-dimensional images, and to characterize and discriminate among tissues based on their physical and biochemical components and the collected MRI information. Therefore, MRI is helpful in diagnosis of parenchymal lesions [1-5]. In addition, unlike computed tomography (CT), general X-ray devices, single photon emission computed tomography (SPECT), and positron emission tomography (PET), MRI requires no exposure to ionizing radiation, has excellent soft tissue contrast and the advantage of being able to take high-resolution vascular images without contrast agents [6-14]. However, because the visual inspection of MRI images is essential for diagnosis of diseases, the improvement of contrast between tissues is important [15]. To this end, we need apply one of various techniques to optimize the MRI parameters [16, 17]. Among these optimization techniques, T1 or T2 weighted images and fluid-attenuated inversion recovery (FLAIR) are useful for detecting lesions [18-22]. In particular, the T2 weighted image is a representative imaging technique using long repetition time (TR) and echo time (TE); its most characteristic feature is that water appears white [23]. Because most lesions contain water, T2 weighted images have good contrast between lesion and normal tissues. Hence, these images are mainly used in the detection of lesions for soft tissues and diagnosis of lesion characteristics [24].

However, setting a long TR or TE is known to delay the image acquisition time. The delayed image acquisition time causes image distortion as a result of the patient's movement [25, 26]. In addition, in the process of converting a magnetic signal into an electrical signal when acquiring an MRI image, noise is generated by a number of external and environmental factors such as the external magnetic field, electrical interference, weak signal strength, and short scan time. Distortion and noise generated in MRI images negatively affect image analysis, such as tissue classification and lesion search, and increases the possibility of misdiagnosis by reducing the accuracy of diagnosis and treatment. Moreover, the distortion and noise in T2 weighted images cause a deterioration in

©The Korean Magnetics Society. All rights reserved.
*Corresponding author: Tel: +82-32-820-4362
Fax: +82-32-822-4449, e-mail: yj20@gachon.ac.kr

© 2021 Journal of Magnetics

image characteristics, thereby reducing the contrast between tissues, which can cause difficulty in detecting lesions. To lower the misdiagnosis rate and improve the reliability of the images, image distortion and noise must be removed. For this purpose, image acquisition techniques have been developed focused on adjusting various parameters. For example, a gradient-echo (GE) technique has been demonstrated that can reduce image distortion via shortening the shooting time by adjusting the flip angle, which is the angle between the macroscopic magnetization vector and the static magnetic field direction [27]. In addition, adjusting the number of excitations (NEX) and bandwidth (BW) can improve the signal-to-noise ratio (SNR) by controlling the amount of noise generated in the image as follows [28]:

$$SNR \propto \sqrt{\frac{(N_y) \times (N_x) \times (NEX)}{BW}}. \quad (1)$$

where N_y refers to the number of phase coding steps, and N_x refers to the number of frequency coding steps. BW is a range of frequencies included in the range between the highest and lowest frequencies allowed for a signal, and NEX refers to the number of repetitions of signal data filled in k-space. Adjusting these parameters, MR images with improved SNR can be obtained. However, few studies have been conducted to suggest well-defined methods or values for optimization [29].

Therefore, the objective of this study is to find the optimal parameters for MRI images, which were acquired by fixing all parameters and sequentially changing the flip angle, NEX, and BW.

2. Materials and Methods

2.1. Acquiring T2 weighted images using MRiLab simulation program

The modeled MRiLab simulation program (ver. 1.3, USA) was modeled by University of Wisconsin at Madison based on environment similar to real MRI device (GE Discovery MR750, GE Healthcare, USA). This program is a user-friendly software toolset, can be used to acquire MRI images in a short time by adjusting various sequences and parameters using a simple operation [30]. In this study, the flip angle, NEX, and BW were sequentially changed to acquire simulated T2 weighted images of the human brain after setting all the parameters of the MRI using this MRiLab simulation program. The flip angle was varied from 10° to 170° at intervals of 20°; NEX was set as 1, 2, 3, 4, 5, 10, 20, 30, 40, and 50, and BW was set as 10, 30, 50, 70, 80, 90, 110, 130, and 160 Hz. TR of 10 s, TE of 0.5 s, and slice thickness of 4 mm were set as fixed parameters. In addition, for quantitative evaluation with similarity factors, a reference image was obtained with parameter values set as 90° flip angle, NEX 50, and BW 10 Hz. Table 1 shows the parameters of the acquired images and the reference image.

2.2. Quantitative evaluation

Noise level and similarity factors were evaluated to quantitatively analyze the tendencies of image characteristics according to the application of various parameters in simulated MRI images. Fig. 1 presents the regions of interest (ROIs) set for noise level evaluation using SNR and contrast-to-noise ratio (CNR). The formulas for SNR and CNR are as follows:

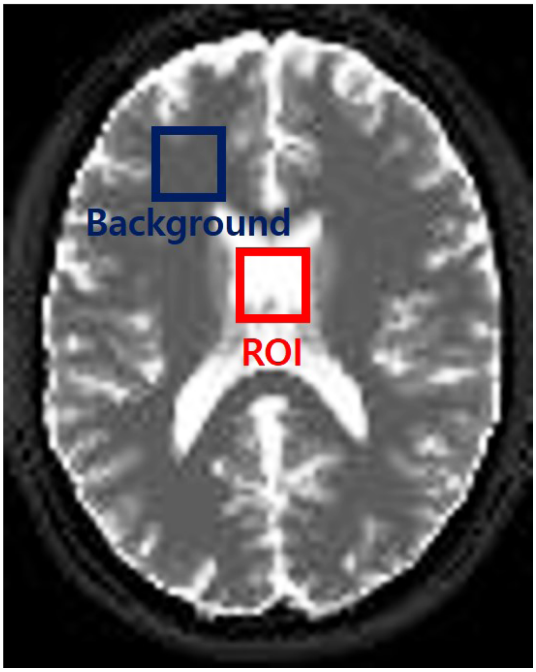

Fig. 1. (Color online) Setting of ROI at the reference image acquired through MRiLab simulation program.

Table 1. Various parameter values set for acquiring MR images with MRiLab simulation program.

	Flip angle	NEX	BW (Hz)	Noise level (%)
Acquired images	From 10° to 170° at 20° intervals	1, 2, 3, 4, 5, 10, 20, 30, 40, 50	10, 30, 50, 70, 80, 90, 110, 130, 160	60
Reference image	90°	50	10	0

$$SNR = \frac{S_A}{\sigma_A}. \tag{2}$$

where S_A is the average value of the signal intensity in the ROI region and σ_A is the standard deviation of the signal intensity. SNR is the signal-to-noise ratio, which is a factor acquired by dividing the average value of the signal strength of the ROI region by the standard deviation of the signal strength. The higher the SNR value, the lower is the noise ratio.

$$CNR = \frac{|S_A - S_B|}{\sqrt{\sigma_A^2 - \sigma_B^2}}. \tag{3}$$

where S_A and S_B represent the average value of the signal intensity in the ROI and background regions, respectively, and σ_A and σ_B represent the standard deviation of the signal intensity in the ROI region and the background region, respectively. CNR is a factor for evaluating the characteristics of an image as a ratio of the noise, analyzing the contrast and noise of the image together and comparing the contrast of the ROI against the ambient noise. The larger the CNR value, the better is the image characteristics.

Moreover, the root mean square error (RMSE), peak signal-to-noise ratio (PSNR), correlation of coefficient (CC), and universal quality index (UQI) were calculated for similarity evaluation.

$$RMSE = \sqrt{\frac{\Sigma_{i=1}^{N}(f_i - g_i)^2}{N}}. \tag{4}$$

where f_i and g_i denotes the original image and the comparison image, respectively, and N denotes the number of pixels in images. RMSE refers to a factor indicating the degree of error occurring between two images. The smaller the RMSE value, the more similar the original image and the reconstructed image are; the larger the value, the lower is the similarity.

$$PSNR = 10\log\left(\frac{S_{peak}}{RMSE}\right)^2. \tag{5}$$

where S_{peak} refers to the value of the signal with the maximum amplitude. PSNR refers to the maximum signal-to-noise ratio between two images, that is, the maximum power of noise in the signal sample. It is used to evaluate the loss of image quality in the process of reconstructing an image. Larger PSNR values indicate less video signal loss.

$$CC = \frac{\Sigma_{i=1}^{N}(f_i - \hat{f})(g_i - \hat{g})}{\sqrt{\Sigma_{i=1}^{N}(f_i - \hat{f})^2}\sqrt{\Sigma_{i=1}^{N}(g_i - \hat{g})^2}}. \tag{6}$$

where $\hat{f}$ and $\hat{g}$ mean the average pixel values of original and comparison images. CC is an evaluation factor linearly measuring the similarity between two images with the

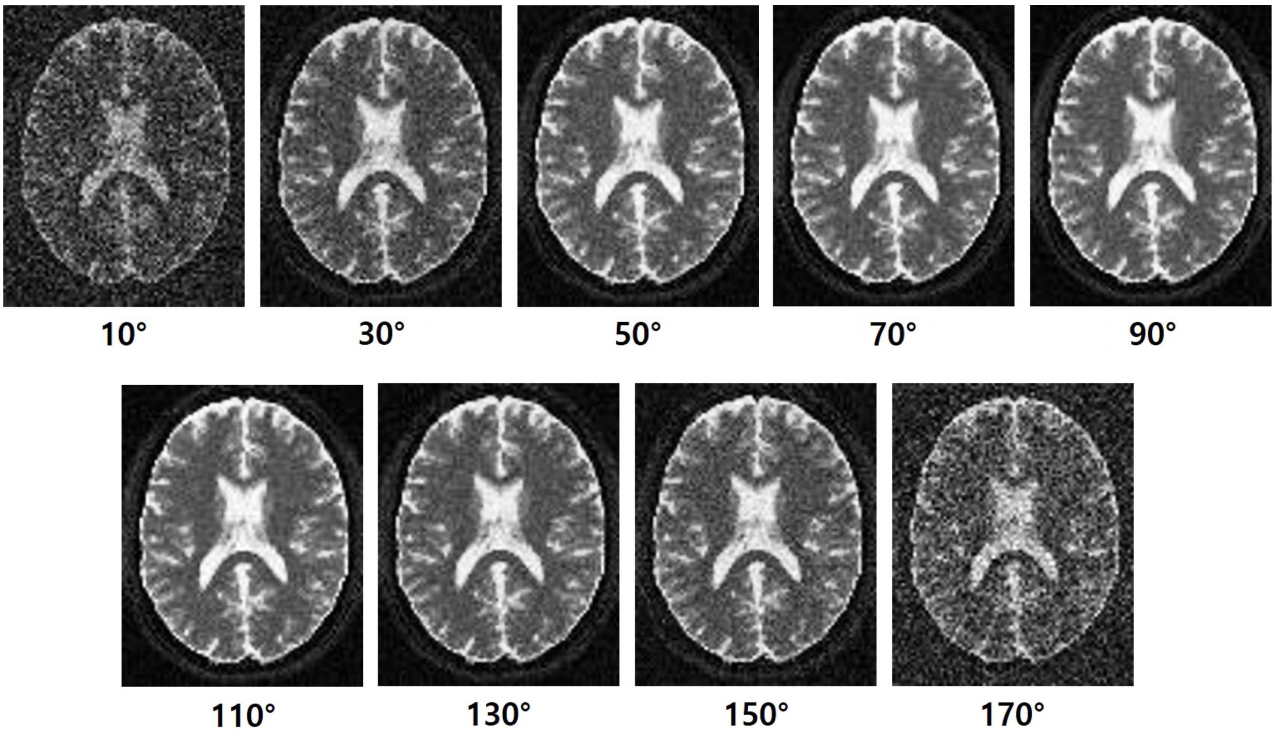

Fig. 2. Brain T2 weighted images acquired by changing the flip angle using MRiLab simulation program.

Pearson correlation coefficient. CC is measured within the range of 0 to 1, and the closer the measured value is to 1, the more similar is the reconstructed image to the original image.

$$UQI = \frac{4\mu_f \mu_g \sigma_{fg}}{(\mu_f^2 + \mu_g^2)(\sigma_f^2 + \sigma_g^2)} . \quad (7)$$

where μ_f and μ_f mean the average luminance values, and σ_{fg} means the covariance between original and comparison image. UQI is a factor that measures and evaluates the similarity between an original image and a reconstructed image. The UQI ranges from 0 to 1, and the closer the measured value is to 1, the more similar is the reconstructed image to the original image.

3. Results

Figure 2 presents T2 weighted neuroimages acquired through the MRiLab simulation program by changing only the flip angle from 20° to 170° at 20° intervals while

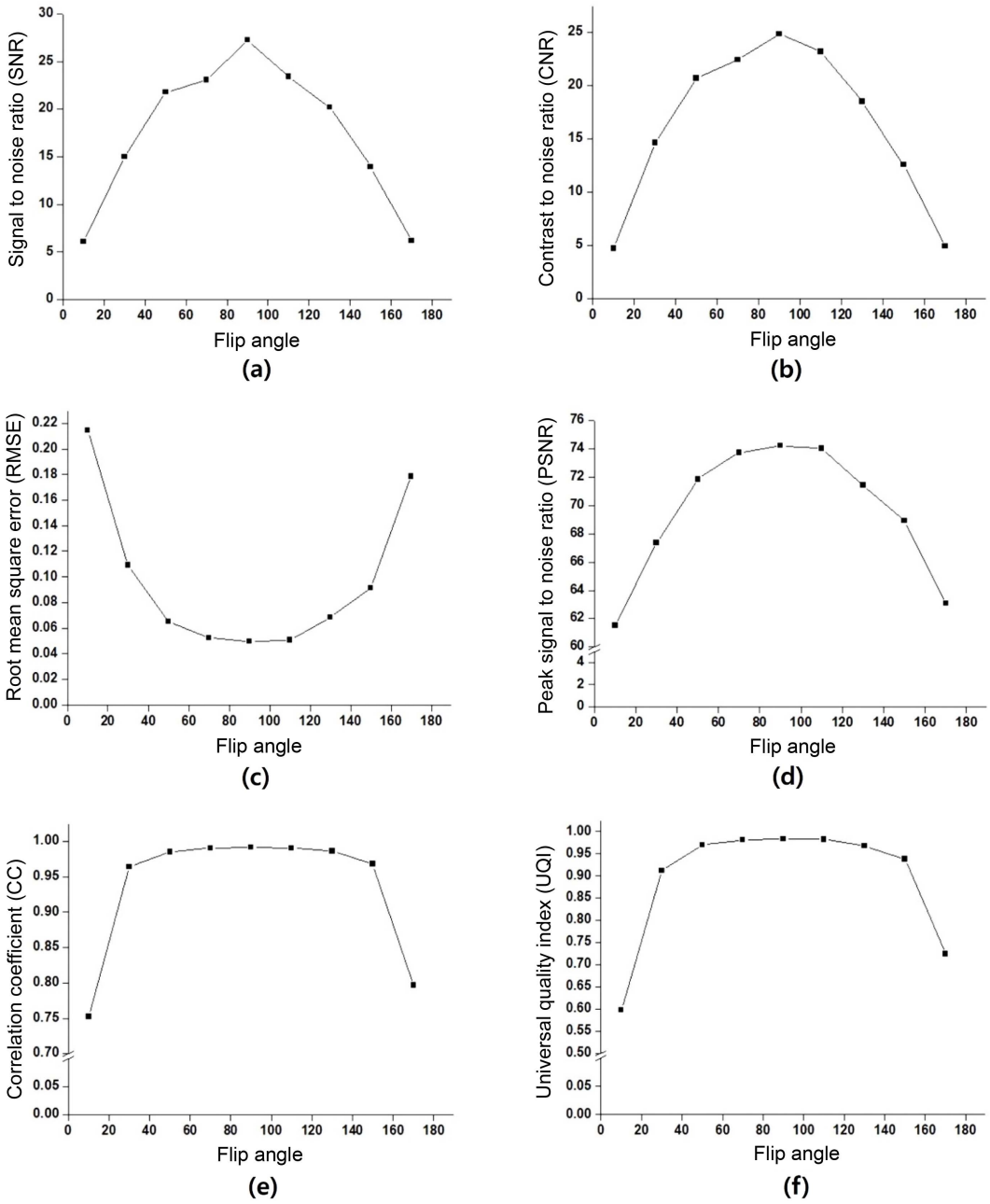

Fig. 3. Quantitative evaluation results of brain T2 weighted images acquired by changing the flip angle: (a) SNR, (b) CNR, (c) RMSE, (d) PSNR, (e) CC, and (f) UQI.

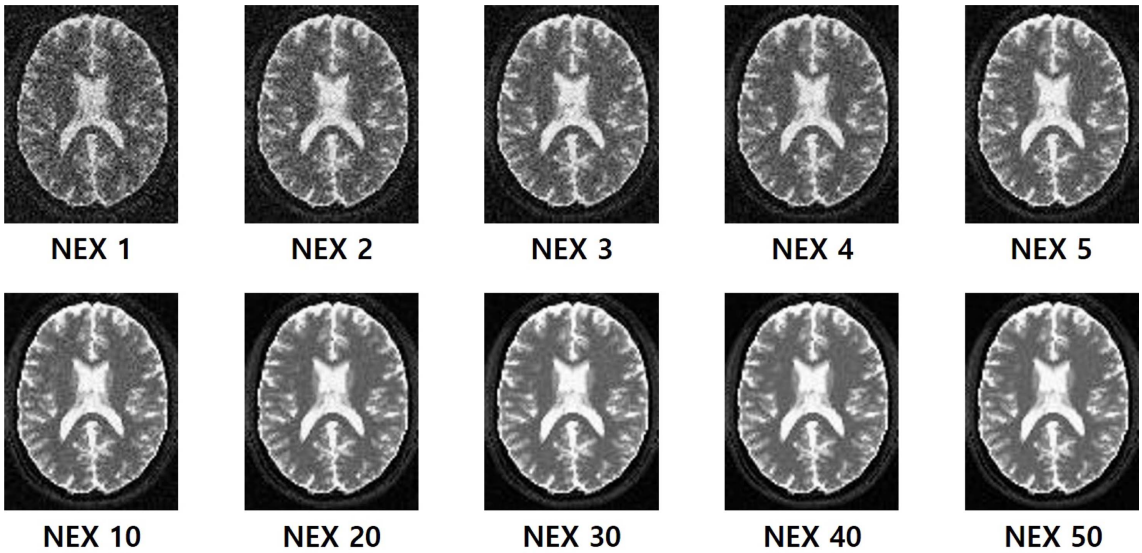

Fig. 4. Brain T2 weighted images acquired by changing the NEX using MRiLab simulation program.

all remaining parameters are fixed. Fig. 3(a) and (b) show the results for SNR and CNR, respectively. The SNR and CNR increased up to a 90° flip angle and then decreased. It can be observed that, visually, the image is best at 90°. The characteristics of the image deteriorate before and after 90°. Fig. 3(c), (d), (e), and (f) present the results of the RMSE, PSNR, CC, and UQI; they show the similarity evaluation results of images acquired by varying the flip angle. The PSNR, CC, and UQI increased up to a 90° flip angle and then decreased; the RMSE decreased up to a 90° flip angle and then increased. In addition, the image at 90° was most similar to the reference image; the similarity of images before and after 90° was reduced.

Figure 4 presents T2 weighted human brain images acquired through the MRiLab simulation program by changing only the NEX from 1 to 5 on 1 interval, and 10 to 50 on 10 intervals, while all remaining parameters are fixed. Fig. 5(a) and (b) show the variations in noise level for the various acquired images on the basis of the calculated SNR and CNR; the figures demonstrate that the SNR and CNR increased as NEX increased. Fig. 5(c), (d), (e), and (f) show the results of the similarity evaluation; as NEX increased, PSNR, CC, and UQI increased and RMSE decreased. Moreover, images with a larger NEX also visually show better image quality.

Figure 6 presents T2 weighted neuroimages acquired by changing only BW while fixing all remaining parameters through the MRiLab simulation program. Fig. 7(a) and (b) show the variations in noise level for the various acquired images on the basis of the calculated SNR and CNR; they show that the SNR and CNR decreased as BW increased. Fig. 7(c), (d), (e), and (f) show the results of the similarity evaluation; as BW increased, PSNR, CC, and UQI decreased and RMSE increased. In particular, the best image characteristics were found at 10 Hz with the smallest BW, and the worst image characteristics at 160 Hz with the highest BW. In particular, lower BW images show visually better image quality.

4. Discussion

MRI medical image acquisition devices are currently very actively used for lesion diagnosis in the clinical field. To improve the characteristics of these MR images, more optimized various parameters should be set. Therefore, in this study, we performed quantitative evaluations of T2 weighted images of the simulated human brain acquired by fixing all parameters in a simulated MRI through the MRiLab simulation program, and varying flip angle, NEX, and BW, to identify the tendency, seeking to find the optimal parameter values.

The flip angle used in this study is the angle between the magnetization vector and the direction of the static field. The flip angle has a close relationship with signal intensity; the formula showing their relationship is as follows [31]:

Signal intensity =

$$M_0 \times \sin(\alpha) \cdot \frac{1 - e^{-R_1 \cdot TR}}{1 - \cos(\alpha) \cdot e^{-R_1 \cdot TR}} \cdot e^{R_2(*)TE}. \quad (8)$$

where M_0 is the strength of gradient, α is the flip angle, R_1 and R_2 are unique characteristics of $_1H$ protons in a given magnetic field. As α approaches 90°, the signal

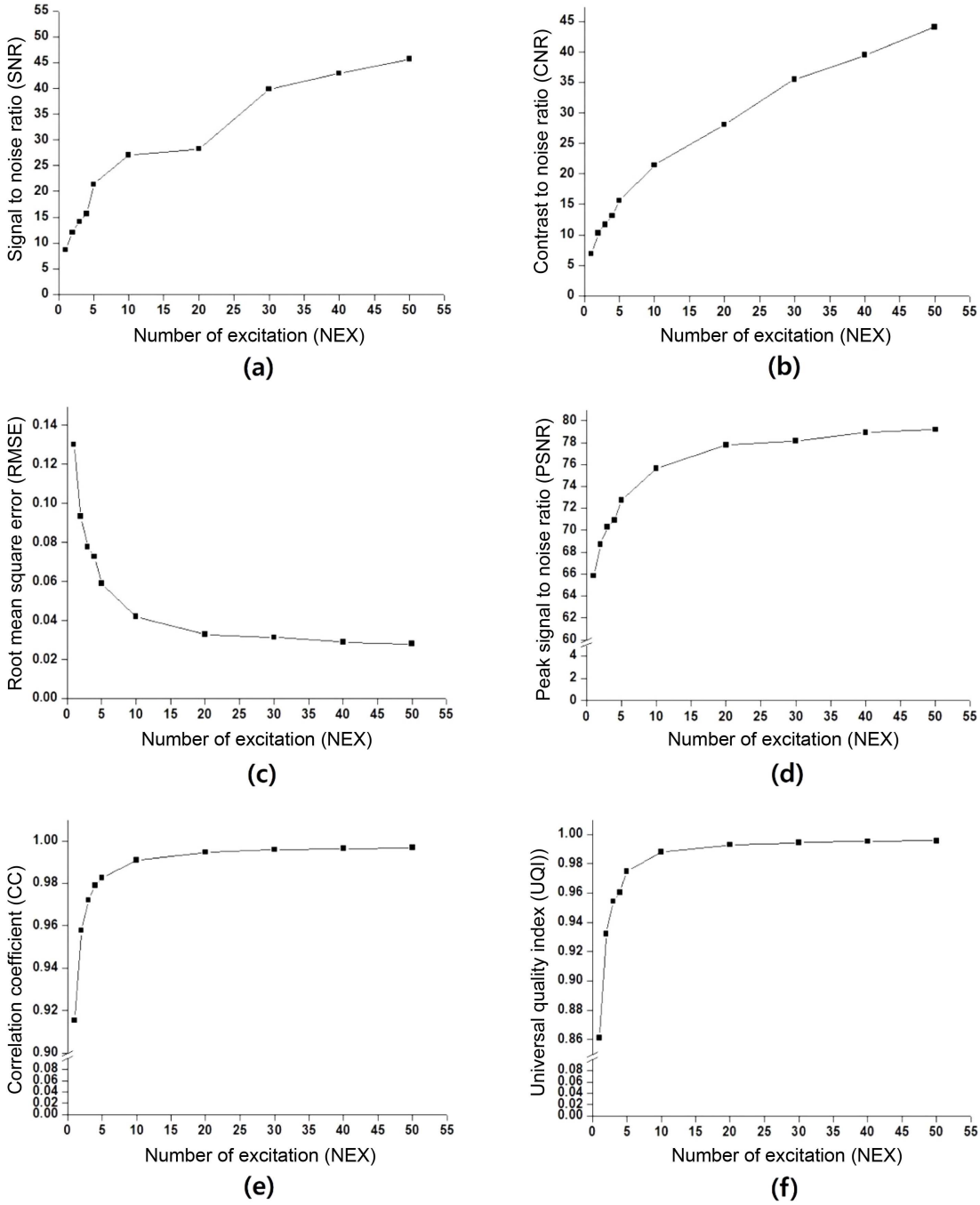

Fig. 5. Quantitative evaluation results of brain T2 weighted images acquired by changing the NEX: (a) SNR, (b) CNR, (c) RMSE, (d) PSNR, (e) CC, and (f) UQI.

intensity becomes stronger, so the signal intensity is the greatest at 90° and it makes the image has the best characteristics at 90°. In the case of 10° with the smallest flip angle, the image characteristics are not good because the signal strength is very small. On the contrary, in the case of 170° with the largest flip angle, during predetermined TR, not only the signal strength very weak due to insufficient recovery, but also the image characteristics may be poor due to the occurrence of a partial volume artifact.

The second parameter used in this study, NEX, is the number of excitations. The techniques for acquiring images by adjusting NEX include fractional NEX and partial NEX techniques. Although the increase in NEX

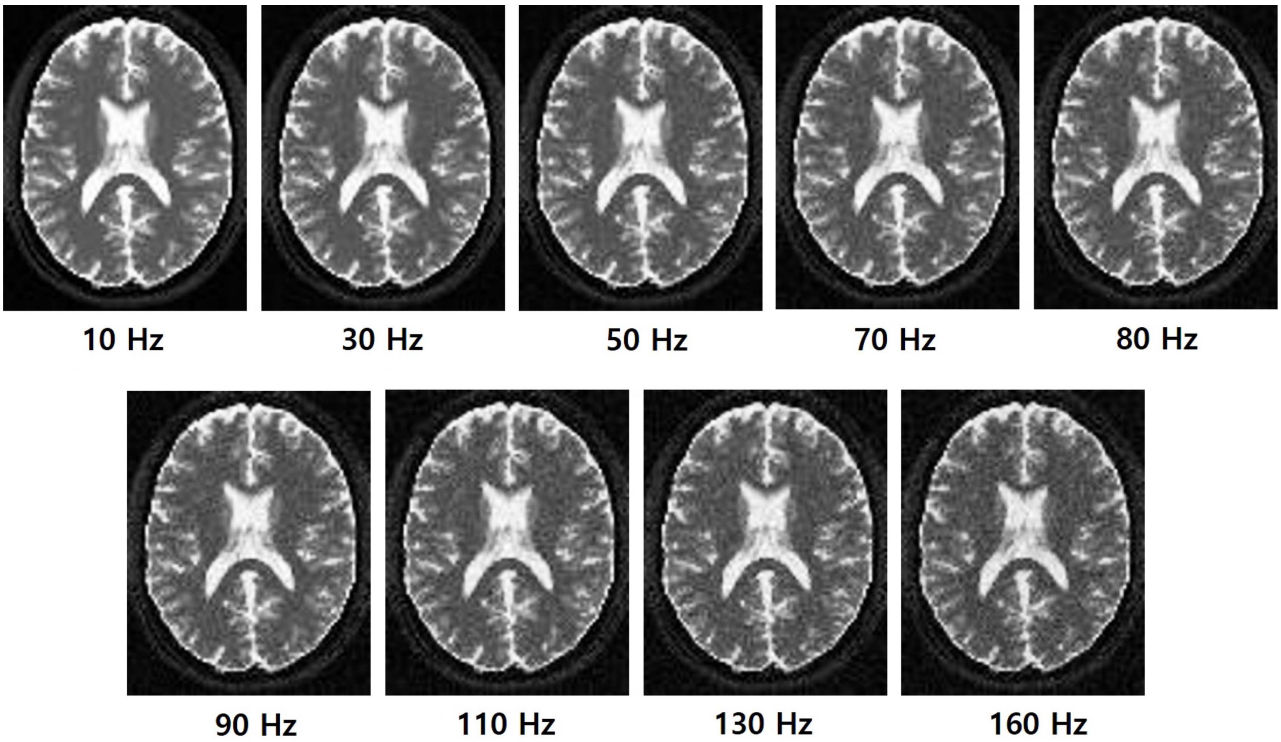

Fig. 6. Brain T2 weighted images acquired by changing the BW using MRiLab simulation program.

improves the characteristics of the MR images, it also causes a problem in that the scan time increases. The formula showing the relationship between NEX and scan time is as follows [32].

$$\text{Scan time} = TR \times N_y \times NEX. \quad (9)$$

where TR is the repetition time, and N_y is the number of phase coding steps. An increase in NEX effectively leads to an improvement in image characteristics; however, an excessively large NEX requires a long scan, which may cause image noise and motion artifacts due to patient movement. In addition, from the quantitative evaluation of the image, we conclude that it is necessary to set an appropriate NEX because the degree of improvement of the image characteristics decreases after an increase in NEX above a certain value.

The third parameter is BW, it means the full receiver bandwidth in this study. As the BW becomes wider, it can decrease the minimum TE, the chemical shift, metal and susceptibility artifacts as well as the increase of bandwidth allows the shorter TR and TE values [33, 34]. However, the SNR decreases and the amount of noise and the minimum field of view increase [34, 35].

As a result, optimization of MRI image parameters such as flip angle, NEX, and BW can improve image characteristics. Excessive increase or decrease from these optimal values cause more noise and artifacts in the image, leading to degradation of image characteristics. Therefore, it was confirmed that it is important to set appropriate parameters when acquiring an MRI image [36-38].

In summary, after fixing all parameters, the experiment was conducted by individually adjusting the flip angle, NEX and BW. Our experimental results are expected to be used as basic data in the process of parameters optimization for various MRI devices that require calibration. However, note that adjusting one parameter can affect other parameters as well. Especially, our experiments were performed only by simulation, and data were not obtained on the simultaneous changes of various parameters even though MRiLab simulation program was modeled similar to real MR device. To overcome these limitations, a follow-up study is needed to confirm the optimal parameter value by adjusting the parameters at the same time rather than adjusting the parameters individually, and then to confirm whether similar results are obtained in actual clinical practice.

5. Conclusion

In this study, after fixing all parameters of MRI, quantitative evaluation was performed on T2 weighted images of the simulated human brain acquired by changing the

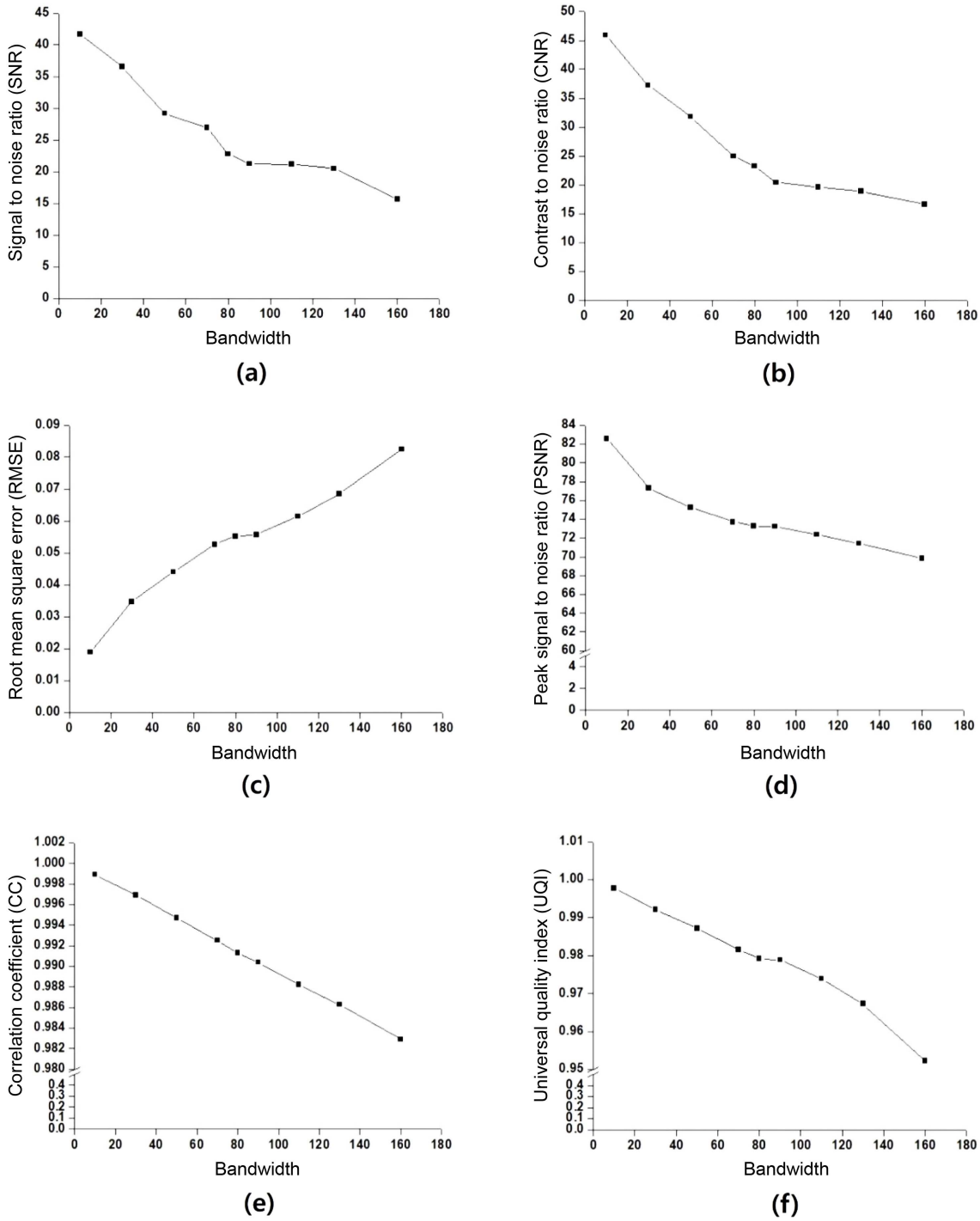

Fig. 7. Quantitative evaluation results of brain T2 weighted images acquired by changing the BW: (a) SNR, (b) CNR, (c) RMSE, (d) PSNR, (e) CC, and (f) UQI.

various parameters; then, the tendency was analyzed. As a result, the 90° flip angle, NEX 50 and BW 10 Hz showed the best characteristics. However, the unsuitable setting of parameters can cause deterioration of image characteristics. Hence, it was confirmed that it is important to set appropriate parameters when acquiring T2 weighted images of the brain.

Acknowledgement

This work was also supported by the Gachon University research fund of 2020 (GCU-2020-02850001).

References

[1] L. C. Ho, I. A. Sigal, N. J. Jan, X. Yang, Y. V. D. Merwe, Y. Yu, Y. Chau, C. K. Leung, I. P. Conner, T. Jin, E. X. Wu, S. G. Kim, G. Wollstein, J. S. Schuman, and K. C. Chan, Scientific Reports **6**, 1 (2016).

[2] E. K. Fram, R. J. Herfkens, G. A. Johnson, G. H. Glover, J. P. Karis, A. Shimakawa, T. G. Perkins, and N. J. Pelc, Magn. Reson. Imaging **5**, 201 (1987).

[3] M. Danaci, T. Akpolat, M. Koyuncu, R. Ünal, and Ü. Belet, Comput. Med. Imaging Graph. **24**, 121 (2000).

[4] Y. Han, J. Korean Phys. Soc. **68**, 467 (2016).

[5] O. Cetin, V. Seymen, and U. Sakoglu, Inform. Med. Unlocked **20**, 100409 (2020).

[6] G. Antoch and A. Bockisch, Eur. J. Nucl. Med. Mol. Imaging **36**, 113 (2009).

[7] R. Sinha, P. Murphy, P. Hawker, S. Sanders, A. Rajesh, and R. Verma, Clin. Radiol. **64**, 341 (2009).

[8] V. Sheejakumari and B. S. Gomathi, Computational and Mathematical Methods in Medicine, Electronics and Mechatronics Engineering, (2015).

[9] T. Ai, J. N. Morelli, X. Hu, D. Hao, F. L. Goerner, B. Ager, and V. M. Runge, Invest. Radiol. **47**, 725 (2012).

[10] R. C. Semelka, D. M. Armao, J. E. Junior, and W. Huda, Journal of Magnetic Resonance Imaging: an Official Journal of the International Society for Magnetic Resonance in Medicine **25**, 900 (2007).

[11] Y. Fujinaga, C. Lall, A. Patel, T. Matsushita, R. Sanyal, and M. Kadoya, Insights Into Imaging **4**, 321 (2013).

[12] E. H. Goo, D. C. Kweon, K. R. Dong, J. S. Lee, W. K. Chung, J. Choi, J. W. Lee, and C. H. Choe, Appl. Magn. Reson. **40**, 221 (2011).

[13] R. Misri, K. Saatchi, and U. O. Häfeli, Nanomedicine **7**, 719 (2012).

[14] M. A. Balafar, A. R. Ramli, M. I. Saripan, and S. Mashohor, Artif. Intell. Rev. **33**, 261 (2010).

[15] D. C. Chang and W. R. Wu, IEEE Trans. Med. Imaging **17**, 518 (1998).

[16] C. H. Yang, S. H. Hong, J. C. Jao, S. N. Tsai, C. C. Shiao, K. W. Yeung, and P. C. Chen, Biomarkers and Genomic Medicine **5**, 39 (2013).

[17] K. Hittmair, G. Gomiscek, K. Langenberger, M. Recht, H. Imhof, and J. Kramer, Magn. Reson. Med. **31**, 567 (1994).

[18] P. Sati, I. C. George, C. D. Shea, M. I. Gaitán, and D. S. Reich, Radiology **265**, 926 (2012).

[19] J. G. Adams and E. R. Melhem, AJR. Am. J. Roentgenol. **172**, 529 (1999).

[20] J. K. Lee, H. Y. Choi, S. W. Lee, S. Y. Baek, and H. Y. Kim, Clinical Imaging **24**, 263 (2000).

[21] R. Bakshi, S. Ariyaratana, R. H. B. Benedict, and L. Jacobs, Archives of Neurology **58**, 742 (2001).

[22] H. Isoda, S. Arizono, K. Shimada, Y. Hirokawa, Y. S. Maetani, M. Kataoka, Y. Nakamoto, T. Shibata, and K. Togashi, Clinical Imaging **35**, 133 (2011).

[23] P. Bannas, U. Motosugi, S. Ichikawa, D. Hernando, and S. B. Reeder, Clinical Liver Disease **4**, 120 (2014).

[24] B. M. Kline-Fath, M. A. Calvo-Garcia, S. M. O'Hara, and J. M. Racadio, Pediatric Radiology **37**, 133 (2007).

[25] Y. Ohgiya, J. Suyama, N. Seino, S. Takaya, M. Kawahara, M. Saiki, S. Sai, M. Hirose, and T. Gokan, J. Magn. Reson. Imaging **32**, 1061 (2010).

[26] L. Xiang, Y. Chen, W. Chang, Y. Zhan, W. Lin, Q. Wang, and D. Shen, International Conference on Medical Image Computing and Computer-Assisted Intervention 215 (2018).

[27] M. C. Hedberg, B. P. Drayer, R. A. Flom, J. A. Hodak, and C. R. Bird, Am. J. Neuroradiol. **9**, 145 (1988).

[28] J. P. Dillenseger, S. Molière, P. Choquet, C. Goetz, M. Ehlinger, and G. Bierry, Skeletal Radiol. **45**, 677 (2016).

[29] F. H. Epstein, J. P. Mugler III, and J. R. Brookeman, Magn. Reson. Med. **31**, 164 (1994).

[30] F. Liu, J. V. Velikina, W. F. Block, R. Kijowski, and A. A. Samsonov, IEEE Trans. Med. Imaging **36**, 527 (2016).

[31] H. K. Jeong, K. H. Lee, M. H. Kim, S. H. Kim, M. G. Kim, and H. C. Kim, Appl. Sci. **8**, 1138 (2018).

[32] K. R. Dong, E. H. Goo, J. S. Lee, W. K. Chung, and Y. J. Kim, J. Korean Phys. Soc. **64**, 1202 (2014).

[33] T. B. Parrish, D. S. Fieno, S. W. Fitzgerald, and R. M. Judd, Magn. Reson. Med. **38**, 653 (1997).

[34] J. Graessner, Magnetom Flash **2**, 3 (2013).

[35] A. P. Toms, C. Smith-Bateman, P. N. Malcolm, J. Cahir, and M. Graves, Clin. Radiol. **65**, 447 (2010).

[36] D. Tamada, M. L. Kromrey, S. Ichikawa, H. Onishi, and U. Motosugi, Magn. Reson. Med. Sci. **19**, 64 (2020).

[37] B. Lorch, G. Vaillant, C. Baumgartner, W. Bai, D. Rueckert, and A. Maier, J. Med. Eng., 2017 (2017).

[38] C. A. Park, S. B. Yang, K. J. Lee, Y. B. Lee, H. G. Kim, and C. K. Kang, J. Korean Phys. Soc. 718 (2019).